LA-UR-06-8338

Approved for public release;
distribution is unlimited.

Title:	Plutonium and Neptunium Speciation and Mobility in Soils and the Subsurface
Author(s):	Stephen A. Stout Sean D. Reilly Mary P. Neu
Intended for:	DOE

Los Alamos
NATIONAL LABORATORY
EST.1943

Form 836 (7/06)

Purpose

The DOE is conducting cleanup and stabilization activities at its nuclear weapons development sites, many of which have accumulated plutonium in soils for 60 years. To properly control Pu migration in soils and groundwaters within Federal sites and onto public lands, better evaluate the public risk, and design effective remediation strategies, a fundamental understanding of Pu speciation and environmental transport is needed. The DOE is increasingly relying on monitored natural attenuation (MNA) for site stewardship. While this is practical, and defensible based on fundamental actinide chemistry and most environmental data, there are significant gaps in the foundation of the approach. Key among them is the inability to project migration rates and redistribution of actinide contaminants, particularly given the diversity and heterogeneity of sites. Matrix sorption/desorption processes are the main factors that determine contaminant transport, but little data of this type are available for Pu or Np with minerals and sediments. To support MNA and predictive geochemical models we conducted the following research: 1) Studied environmentally relevant Pu and Np species. 2) Determined the mechanisms and thermodynamics of interactions of Pu and Np species with Mn and Fe (oxy)hydroxides and with sediments, including actinide sorption/desorption during mineral formation and redox cycling.

Research Progress and Implications

I. Plutonium Complexes and Speciation

Pu(VI) Hydroxides, Carbonates, and Chlorides. Plutonium has a rich redox chemistry and can exist in the environment in the four oxidation states, III through VI. Each oxidation state has unique solubility and complexation chemistry that dictates its behavior in the environment.[1] It is therefore important that geochemical models of actinide transport in contaminated environments include accurate information on the redox speciation of Pu. Plutonium has low solubility in most aqueous systems at near-neutral pH and exists primarily as tetravalent (hydr)oxides. The small fraction of total Pu that is soluble often consists of pentavalent and hexavalent molecular complexes and suspended colloids. For many years, our research team has been active in the study of fundamental and environmental actinide chemistry.

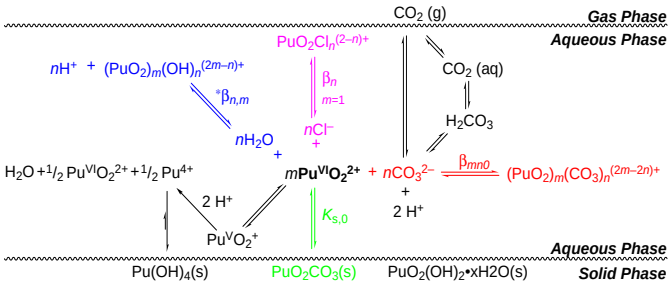

Figure 1: Numerous Pu(VI) species can exist in aqueous solution. Complexation, solubility, sorption, and redox equilibria exist.

We have used a variety of experimental techniques to investigate some of the environmentally-relevant equilibria shown in Figure 1. We studied the chloride complexation of Pu(VI) in NaCl media using visible-near infrared (vis-NIR) spectrophotometry and determined the stability constants of the PuO_2Cl^+ and $PuO_2Cl_2^0$(aq) complexes.[2] The initial hydrolysis of Pu(VI) was

studied using complementary potentiometric and vis-NIR techniques to collect data similar to Figure 2 as a function of Pu concentration.[3] We found evidence for both monomeric and dimeric initial hydrolysis species, depending upon the Pu(VI) concentration. At sub-millimolar Pu concentrations (< 10^{-4} M), mononuclear species of the form $PuO_2(OH)_n^{(2-n)+}$ are present in solution. At higher concentrations dimeric Pu(VI) hydrolysis species predominate. In contrast to the behavior of U(VI), polymeric hydrolysis species such as $(PuO_2)_3(OH)_5^+$ were not observed and Pu(VI) monomeric species persist at higher solution concentrations compared to U(VI).

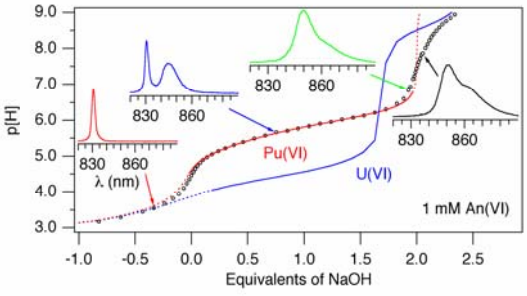

Figure 2: Simultaneous potentiometric and spectrophotometric data collection used to determine Pu(VI) hydrolysis speciation.

We have determined the solubility product of PuO_2CO_3(s) in NaCl and $NaClO_4$ media as a function of electrolyte concentration. For this study, solid PuO_2CO_3 was prepared and characterized using powder XRD and diffuse reflectance spectroscopy. The solid was then equilibrated with NaCl and $NaClO_4$ solutions of various concentrations and then solution vis-NIR spectra were collected (see examples in Figure 3). These spectra show that dissolved Pu(VI) from the solid phase undergoes reduction to Pu(V) at a rate dependent upon the nature of the solution phase. Pu(VI) in low IS carbonate solutions is reduced more rapidly to Pu(V), whereas concentrated NaCl appears to stabilize the higher oxidation state, mainly via chloro complexation and the radiolytic production of hypochlorite. Pu(V) subsequently disproportionates to Pu(VI) and Pu(IV), and the Pu(IV) precipitates as a hydroxide. This process is evident in diffuse reflectance spectra of aged PuO_2CO_3 solids, which show absorbances characteristic of both Pu(VI) carbonate and Pu(IV) hydroxide. Deconvolution of solution spectra enabled us to determine the PuO_2^{2+} solution concentration and the PuO_2CO_3 solubility product in various aqueous solutions.

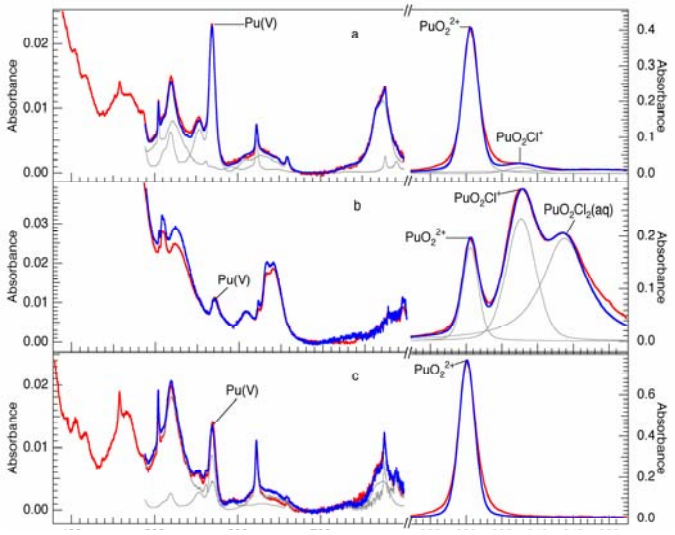

Figure 3: Absorbance spectra shown in red of solution phases from solubility experiments of PuO_2CO_3 in (a) 0.1 m NaCl, (b) 5.6 m NaCl, (c) 5.6 m $NaClO_4$. Shown in grey are the component Pu species used to generate an overall spectra fit shown in blue.

Plutonium solution thermodynamic studies such as these provide valuable data for understanding Pu behavior at the solution–solid interface. As a specific example, Pu(VI)

solution hydrolysis contributes directly to understanding the pH range in which Pu(VI) adsorption to MnO_2 begins (discussed below).

II. Actinide Adsorption onto MnO_2, FeOOH, and Fe_2O_3

Actinide Adsorption by δ-MnO_2: We are also studying the interactions of Pu(V) with minerals. Plutonium associated rapidly with the synthetic mineral phases, regardless of its initial oxidation state. The vis-NIR absorbance spectra for Pu(V) solutions in the presence of δ-MnO_2 are shown in Figure 4. The characteristic absorbance of Pu(V) at 569 nm was not observed; however, a strong characteristic absorbance for Pu(VI) (830 nm) was present showing that Pu(V) was oxidized in solution to Pu(VI). A decrease in intensity of the 830 nm absorbance peak with time indicated the removal of Pu(VI) from solution. Previously, Pu was assumed to associate with MnO_2 phases in a reduced form (III or IV); however, we observed by using X-ray absorption spectroscopy (XAS) that Pu was bound in an oxidized form as a hexavalent inner-sphere complex regardless of the initial Pu oxidation state.

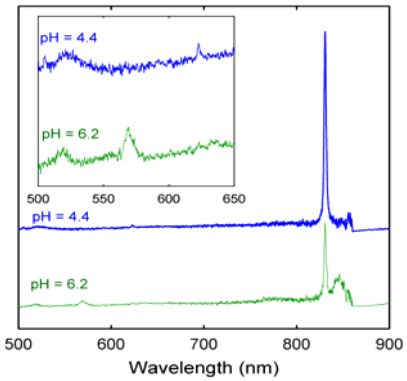

Figure 4. Vis-NIR spectra of Pu(V) solution in contact with MnO_2.

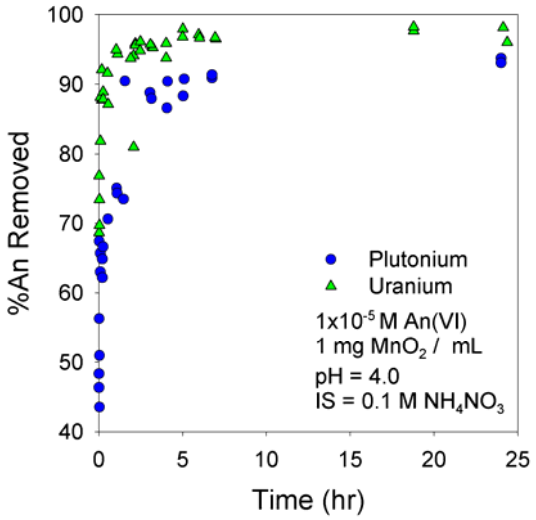

Figure 5. Effect of contact time on Pu(VI) and U(VI) adsorption by δ-MnO_2.

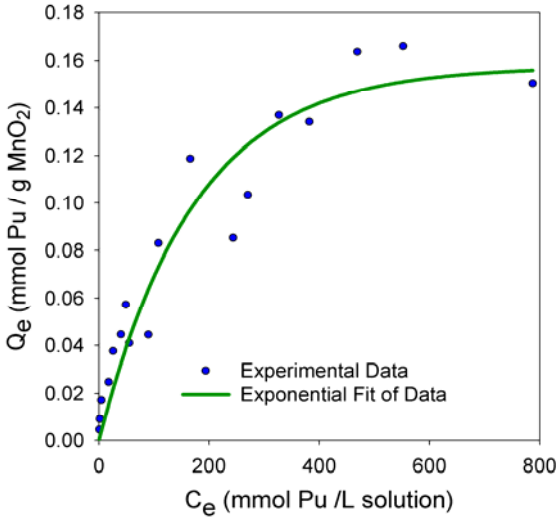

Figure 6. Adsorption capacity of Pu(VI) onto δ-MnO_2 at pH = 4.0.

Batch type experiments were performed to determine the effect of contact time and pH on the adsorption of Pu(VI) and U(VI) by δ-MnO_2 suspended in 0.1 M NH_4NO_3 solutions. Adsorption of Pu(VI) and U(VI) onto δ-MnO_2 as a function of time was studied at pH = 4 and $[AnO_2^{2+}]_{initial}$ = 1 x 10^{-5} M for time periods ranging from a few seconds to several

weeks. Following reaction, the samples were filtered and the An concentration remaining in solution was determined by liquid scintillation counting (LSC). Figure 5 shows the percentages of An(VI) removed from solution for the first 25 hr of reaction. Adsorption of both actinides from solution was characterized by a rapid initial adsorption step, with the majority of the An(VI) removed within the first 5 hr [90% Pu(VI) and 96% U(VI) removed] followed by a much slower adsorption step that occurring over several weeks.

We also conducted a series of experiments to determine the Pu(VI) adsorption capacity of δ-MnO_2 at pH 4.0. This pH was chosen to avoid Pu(VI) hydrolysis and still be at conditions near or above the point of zero charge (PZC) of δ-MnO_2 resulting in a net negative surface charge. Titration experiments were performed by adding aliquots of Pu(VI) to aqueous solutions containing 1 mg δ-MnO_2 / mL. The solutions were allowed to react after each Pu addition and then the concentration of Pu(VI) remaining in the separated solution phase was determined by LSC and vis/NIR spectroscopy. Curve fits of our data resulted in a calculated adsorption capacity of ~0.16 mmol Pu(VI) / g δ-MnO_2 (~10 time less than Cu^{2+}).

Once the effect of time and the adsorption capacity were determined, we set out to study pH-dependence. A 24-hr contact time was used when studying the effect of pH on the adsorption of Pu(VI) and U(VI) by δ-MnO_2 suspended in 0.1 M NH_4NO_3 solutions. The adsorption edges for Pu(VI) were obtained at several initial PuO_2^{2+} concentrations (1.0×10^{-6} to 2.5×10^{-5} M) and were highly pH dependent (Figure 7a). At all concentrations, the %Pu removed increased from near zero at pH = 2 to almost 100% at pH = 4.5. Increasing the initial concentration of Pu(VI) also increases the sorbate/sorbent ratio, resulting in the adsorption edge occurring at a higher pH and a decrease in the percentage of Pu(VI) removed from solution.

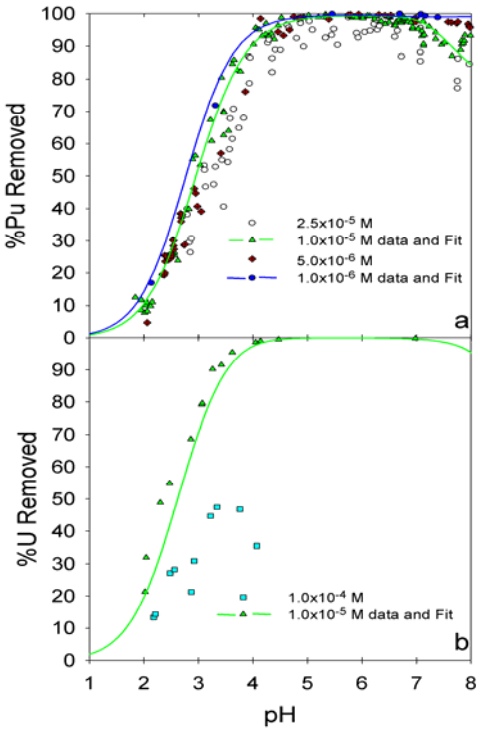

Figure 7. Adsorption edges of Pu(VI) and U(VI) adsorbed onto δ-MnO_2 obtained at $[AnO_2^{2+}]_i = 1\times10^{-6}$ - 1×10^{-4} M.

The Pu(VI) adsorption experiments were repeated utilizing the similar conditions, but in this series we substituted U(VI) at $[UO_2^{2+}]_i = 1\times10^{-6}$ and 1×10^{-4} M. Uranyl adsorption occurred at slightly lower pH than plutonyl, most likely caused by the earlier onset of UO_2^{2+} hydrolysis and the formation of poly-nuclear species at lower concentrations than PuO_2^{2+} (Figure 7b). The adsorption isotherms were generated at total U concentrations and pH values below the region in which schoepite ($UO_2(OH)_2$) precipitates. The percentages of U and Pu removed from solution after 24 hr also agreed well with the

percentages of %An removed from solution at pH 4.0 and $[An]_{initial} = 1\times10^{-5}$ M obtained when the effect of contact time was studied as discussed above.

After gaining an understanding of the Pu(VI)-MnO_2 system, we initiated adsorption studies utilizing hematite and goethite, which are not expect to stabilize Pu(VI) in an oxidized state. Hematite and goethite have very similar binding sites and PZC; therefore, it was not surprising that the actinide adsorption isotherms for a given actinide have very similar pH-dependence and edge positions. Although the surface areas of the mineral suspensions were normalized, the adsorption edges for like actinides were not identical. The adsorption edges for An reacting with goethite occurred at slightly lower pH than those reacting with hematite under similar concentrations. Decreasing the initial concentration of An reacting with the mineral phases also decreased the pH where the adsorption edge occurred. The shape and position of the Pu adsorption edge was more similar to that of the Np(V) than to U(VI), suggesting that the Pu was bound as Pu(V) (Figure 8a). Vis-NIR confirmed that Pu(VI) was reduced to Pu(V) (Figure 8b).

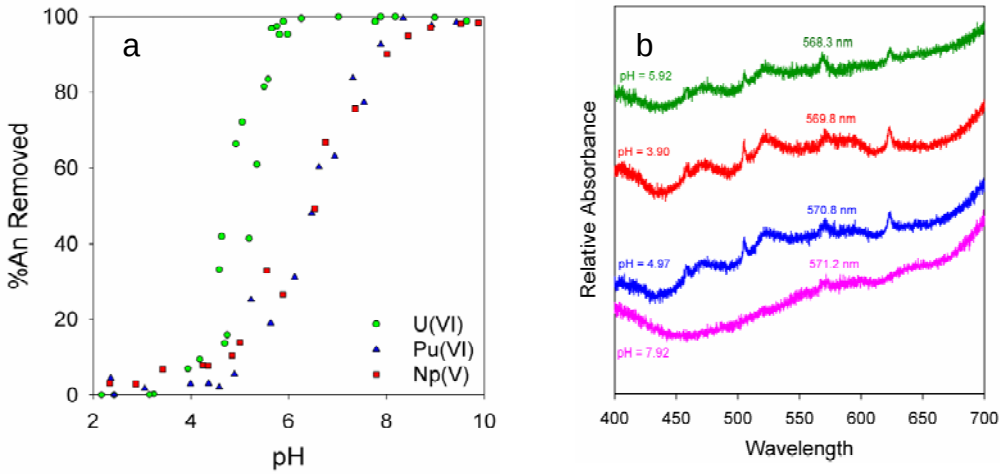

Figure 8 a.) pH dependent adsorption of U(VI), Np(V), and Pu(VI) onto FeOOH. $[An]_{initial} = 10^{-5}$ M, IS = 0.10 M, and 8 mg FeOOH / 10 mL. b.) UV/Vis spectra of Pu(VI) solution in contact with FeOOH. $[Pu(VI)]_{initial} = 10^{-4}$ M and time = 24 h.

These results contrast those observed when studying Pu(V) interactions with δ-MnO_2, as discussed previously. In the presence of δ-MnO_2, Pu(V) was completely oxidized to Pu(VI) and bound to the manganese oxide as a Pu(VI) inner-sphere surface complex. The goethite solids were filtered from the reaction solutions, washed, and air-dried for ~1 month in a glovebox before undergoing analysis with x-ray photoelectron spectroscopy (XPS) (Figure 9). The XPS results indicted that at near-neutral pH, Pu was bound to the mineral surface primarily as Pu(IV) with a small percentage of Pu(V) present. These

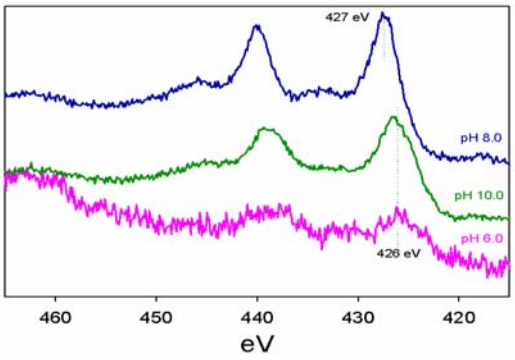

Figure 9. X-ray photoelectron spectroscopy of Pu adsorbed onto hematite.

experiments were conducted under CO_2 free conditions—even at high pH, no carbonate species were detected by XPS. When tested under similar conditions, Np(V) showed no signs of reduction in solution by vis-NIR or on the goethite solid by XPS.

Surface Complexation Modeling of Pu(VI) and U(VI) Reacted with δ-MnO_2: We used a simple single-site non-electrostatic surface complexation model (SCM) to fit our experimental data from the Pu(VI) and U(VI) pH-dependent adsorption isotherms. Input data consisted of thermodynamic solution speciation constants and the BET-N_2 surface area. Surface site concentrations and surface protonation constants were calculated from these data. A site density of 0.67 sites / nm^2 (1.11 μmol / m^2) was determined by fitting the product of the experimentally determined BET-N_2 surface area and the site density using the SCM. Table 1 shows the physical properties of the δ-MnO_2 and intrinsic acidity constants fit by the model. We used one type of binding site, and made the assumption when calculating K^{int} that all binding sites were energetically equivalent. Binding sites arose from the amphoteric ionization reactions of surface functional groups (>MnOH) from the uptake and release of protons, according to the reactions:

$$>MnOH_2^+ \leftrightarrow >MnOH + H^+ \quad K^{int}_{a1} \tag{1}$$

$$>MnOH \leftrightarrow >MnO^- + H^+ \quad K^{int}_{a2} \tag{2}$$

where K^{int}_{a1} and K^{int}_{a2} are intrinsic acidity constants determined at zero surface charge and potential.

An extremely good fit of the experimental data was achieved using three surface complexes and a one-site model for PuO_2^{2+} adsorption (Figure 10). The experimental data were initially fit using the percentage of Pu(VI) adsorbed at $[PuO_2^{2+}] = 1\times10^{-5}$ M, and then the intrinsic binding constants were refined using the 1×10^{-6} M data. Table 2 shows the refined intrinsic binding constants for the Pu and U surface complexes used in the SCM. At other concentrations, the fits were calculated using the initial actinyl concentrations and the refined intrinsic binding constants. The surface complexes utilized in the model were related to the surface charge of the δ-MnO_2 and the hydrolysis species of PuO_2^{2+} at different pH values. These surface reactions are described by reactions 3-4.

Table 1. Parameters used to fit adsorption data.

Physical Properties of MnO_2		
BET: 41.1 m^2/g		
Site density: 0.70 sites / nm^2		
pH_{PZC}: 1.67		
Specie	**Surface Acidity Composition**	**Intrinsic Acidity Constants Log K**
$>Mn^{(IV)}O^-$	$Mn^{(IV)}OH, -H^+$	-5.40
$>Mn^{(IV)}OH_2^+$	$Mn^{(IV)}OH, +H^+$	-3.00

$$>MnO^- + PuO_2^{2+} + H_2O \leftrightarrow >MnOPuO_2OH + H^+ \tag{3}$$

$$>MnO^- + PuO_2^{2+} \leftrightarrow >MnOPuO_2^+ \tag{4}$$

Due to the low PZC of δ-MnO_2, surface complexes involving >$MnOH_2^+$ and >$MnOHPuO_2^{2+}$ were not necessary to achieve an accurate fit. The fits also reflect the observed shift in the adsorption edge to higher pH as the initial concentration of Pu is increased.

Based on the hydrolysis and speciation data for uranyl for concentrations (1×10^{-6} M – 1×10^{-4} M) and a pH range (2-6), the predominant solution species in these experiments are UO_2^{2+}, UO_2OH^+, and $(UO_2)_3(OH)_5^+$. Schoepite ($UO_2(OH)_2$) was allowed to supersaturate in the model. However, the experimental data were obtained at U concentrations or pH below the region at which schoepite precipitates. The surface complex, >$MnO(UO_2)_3(OH)_5$, makes up only a small percentage of the U bound to the δ-MnO_2; however, the complex was necessary to constrain the fit. As An ions bind to the oxide surface the concentration of An remaining in solution decreases and shifts the pH where hydrolysis occurs in the system higher (Figure 10). Binding of hydrolyzed species occurs above the pH at which solution hydrolysis is known to occur in systems containing no mineral phases. This phenomenon is partially due to the decrease in solution concentration and the resulting shift in the onset of hydrolysis to higher pH.

Table 2. Intrinsic binding constants for the Pu and U surface complexes used in the SCM.

Specie	Surface Complexation Model Composition	Log K
>$MnOPuO_2^+$	>MnOH, +PuO_2^{2+}, -H^+	1.85
>$MnOPuO_2OH$	>MnOH, +PuO_2^{2+}, -2H^+, +H_2O	-5.09
>$MnOPuO_2(OH)_2^-$	>MnOH, +PuO_2^{2+}, -3H^+, +2H_2O	-13.84
>$MnOUO_2^+$	>MnOH, +UO_2^{2+}, -H^+	2.24
>$MnOUO_2OH$	>MnOH, +UO_2^{2+}, -2H^+, +H_2O	-2.43
>$MnO(UO_2)_3(OH)_5$	>MnOH, + 3UO_2^{2+}, -10H^+, +5H_2O	-16.41

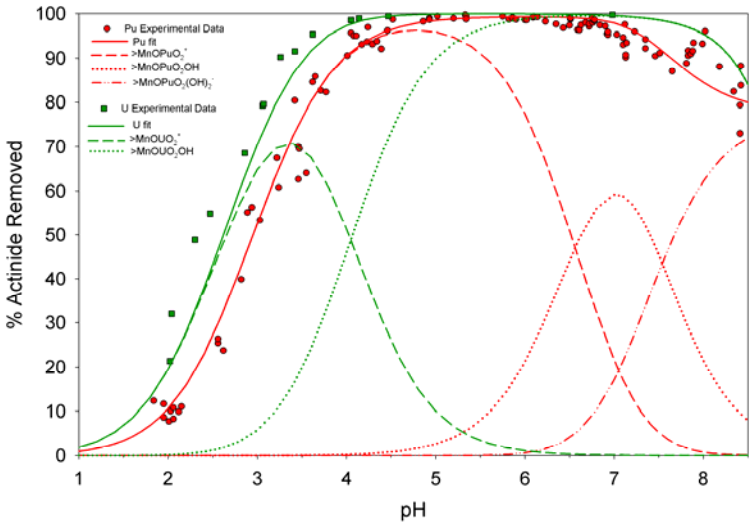

Figure 10. The experimental adsorption data and the fit of the data using the surface complexation model at $[PuO_2^{2+}]_{initial} = 1.0\times10^{-5}$ M in the pH range of 2-8.5.

Initial attempts to prepare fits of the experimental data for Pu(VI) adsorption onto the Fe minerals required the use of two Pu(IV) and two Pu(VI) complexes. Further, the results for Pu adsorption onto iron oxides reflect the differences in the redox behavior between Pu and U, reinforcing the conclusion that there are no functional or structural analogs for Pu environmental chemistry.

Implications and Future Work:

We have studied Pu solution chemistry necessary to improve the accuracy of geochemical models for the prediction of actinide transport in contaminated environments. We have also studied the mechanisms and thermodynamics of Pu and Np interactions with iron and manganese oxide/oxyhydroxides. Actinide removal from solution by δ-MnO_2, FeOOH, and Fe_2O_3 was highly pH dependent. A correlation between adsorption and An hydrolysis was also evident. We were also able to achieve an accurate fit our δ-MnO_2 isotherm data using only Pu(VI) surface complexes. Unlike δ-MnO_2, FeOOH and Fe_2O_3 will not stabilize Pu(VI), but in fact reduce it in solution to Pu(V). We plan to build upon these studies by investigating An desorption rates under similar conditions and expanded these studies to include contaminated sediments from DOE-sites.

References:

[1] Choppin, G. R.; Bond, A. H.; Hromadka, P. M. *Journal of Radioanalytical and Nuclear Chemistry* **1997,** *219*, 203-210.

[2] Runde, W.; Reilly, S. D.; Neu, M. P. *Geochimica et Cosmochimica Acta* **1999,** *63*, 3443-3449.

[3] Reilly, S. D.; Neu, M. P. *Inorganic Chemistry* **2006,** *45*, 1839-1846.

Information Access

Publications

Stout, S.A., S.D. Reilly, D.M. Smith, P.C. Lichtner, and M.P. Neu. (submitted). Plutonium (VI) and uranium (VI) adsorption onto δ-MnO_2; Experimental study and surface complexation modeling. *Environmental Science and Technology.*

Smith, D.M., S.A. Stout, M.A. Ginder-Vogel, S. Skanthakumar, L. Soderholm, and M.P. Neu. (submitted). Plutonium (IV and V) and neptunium (V) oxidation by manganese dioxide. *Journal of Colloid and Interface Sciences.*

Stout, S.A., S.D. Reilly, P.C. Lichtner, and M.P. Neu. 2006. Oxidation and surface complexation of actinyl species by oxides. *Recent Advances in Actinide Science.* eds. I. May, R. Alvares, and N. Bryan. The Royal Society Chemistry, Cambridge, UK. 146-148.

Reilly, S.D., M.P. Neu. 2006. Pu(VI) hydrolysis: Further evidence for a dimeric plutonyl hydroxide and contrasts with U(VI) chemistry. *Inorganic Chemistry*, 45, 1839-1846.

Boukhalfa, H., S. D. Reilly, W. H. Smith, and M. P. Neu. 2004. EDTA and Mixed Ligand Compleses of Tetra- and Trivalent Plutonium, *Inorganic Chemistry*, 43, 5816-1823.

Farr, J.D., R.K. Schulze, M.P. Neu. 2004. Surface Chemistry of Pu Oxides, *J. Nuclear Materials*, 328(2-3), 124-136.

Burns, C.J., M. P. Neu, H. Boukhalfa, K. E. Gutowski, N. J. Bridges, R. D. Rogers. 2004. The Actinides, *Comprehensive Coordination Chemistry II, 3,* 189-345.

Conradson, S.D., Abney, K.D., Begg, B.D., Brady, E.D., Clark, D.L., Den Auwer, C., Ding, M., Dorhout, P.K., Espinosa-Faller, F.J., Gordon, P.L., Haire, R.G., Hess, N.J., Hess, R.F., Keogh, D.W., Lander, G.H., Lupinetti, A.J., Morales, L.A., Neu, M.P., Palmer, P.D., Paviet-Hartmann, P., Reilly, S.D., Runde, W.H., Tait, C.D.; Veirs, D. K., Wastin, F. 2004. Higher Order Speciation Effects on Plutonium L3 X-ray Absorption Near Edge Spectra, *Inorganic Chemistry*, 43(1), 116-131.

Farr, J.D., R.K. Schulze, M.P. Neu. 2004. Surface Chemistry of Pu Oxides, *Actinide Research Quarterly*, 3rd Quarter.

Stout, S.A., S.D. Reilly, D.M. Smith, M.P. Neu. 2004. Pu(V) removal from solution by oxidation and adsorption onto manganese dioxide. *WRI-11 Water Rock Interaction Vol. 1*, eds. R.B. Wanty and R.R. Seal II, 709-713.

Stout, S.A., S.D. Reilly, D.M. Smith, W.K. Myers, M.A. Ginder-Vogel, M.P. Neu. 2003. Interactions of plutonium (V) and plutonium (VI) with manganese dioxide, iron

oxide, and sediments from the Hanford Site. *Plutonium Futures - The Science*. 381-383.

Reilly, S.D., W.K. Myers, S.A. Stout, D.M. Smith, M.A. Ginder-Vogel, and M.P. Neu. 2003. Plutonium (VI) sorption to manganese dioxide. *Plutonium Futures - The Science*. 375-376.

Presentations

"Actinide Intractions with Iron Oxide/Oxyhydroxide." Stout, S.A.; Bauer, E.; Lichtner, P.; Farr, J.D.; Neu, M.P. 4rd Plutonium Futures - The Science Conference, Pacific Grove, CA, July 9-14, 2006.

"*Plutonium Speciation in Environmental Systems, From Hydrolysis to Aerobic and Anaerobic Biogeochemistry.*" Neu, M.P.; Reilly, S.D., Runde, W.; Stout, S.A.; Boukhalfa., H. 4rd Plutonium Futures - The Science Conference, Pacific Grove, CA, July 9-14, 2006.

"Uranyl and Plutonyl Interactions with δ-MnO_2." Bauer, E.; Stout, S.A.; Reilly, S.D.; Lichtner, P.C.; Neu, M.P. American Chemical Society Meeting, Atlanta, Ga, March 27-31, 2006.

"Plutonium (VI) Adsorption onto Hematite, Manganese Oxide, and Quartz." Stout, S.A.; Reilly, S.D.; Lichtner, P.C.; Neu, M.P. Actinides 2005, Manchester, U.K., July 3-8, 2005.

"Actinide Interactions with Redox-Active Minerals." Stout, S.A.; Reilly, S.D.; Smith, D.M.; Neu, M.P. Post Doctoral Poster Session; Los Alamos National Laboratory, June 22, 2005.

"Actinide Adsorption by Manganese Oxide Materials." Stout, S.A.; Reilly, S.D.; Smith, D.M.; Neu, M.P. Chemistry Division Review Committee Poster Session; Los Alamos National Laboratory, Mar. 2005.

"Pu(V) Removal from Solution by Oxidation and Adsorption onto Manganese Dioxide." Stout, S.A.; Reilly, S.D.; Smith, D.M.; Neu, M.P., The Eleventh International Symposium on Water Rock Interaction, Saratoga Springs, N.Y., July 2-6, 2004.

"Interactions of Plutonium (V) and Plutonium (VI) with Manganese Dioxide, Iron Oxide, and Sediments from the Hanford Site." Stout, S.A.; Reilly, S.D.; Smith, D.M.; Myers, W.K.; Ginder-Vogel, M.A.; Neu, M.P., 3rd Plutonium Futures - The Science Conference, Albuquerque, NM, July 6-10, 2003.

"Plutonium (VI) Sorption to Manganese Dioxide." Reilly, S.D.; Myers, W.K.; Stout, S.A.; Smith, D.M.; Ginder-Vogel, M.A.; Neu, M.P., 3rd Plutonium Futures - The Science Conference, Albuquerque, NM, July 6-10, 2003.